

HERMES Measurement of DVCS from p and d Targets, and Status and Prospects of the Recoil Detector

A. Mussgiller (on behalf of the HERMES collaboration)

University of Erlangen-Nuremberg - 91058 Erlangen - Germany

The Deeply Virtual Compton Scattering (DVCS) process provides the theoretically cleanest access to the unknown generalized parton distributions (GPDs). DVCS amplitudes can be measured through the interference between the Bethe-Heitler DVCS processes via the dependence of cross-section asymmetries on the azimuthal angle. The accumulated HERMES data offers access to the four GPDs in different combinations of beam charge and helicity as well as target spin. A recent highlight has been the transverse target-spin asymmetry that provides access to the total angular momentum of quarks.

In late 2005, a Recoil Detector was installed at HERMES with the purpose of greatly improving the experiment's ability to measure hard-exclusive processes during its final running period [1].

1 Introduction

The formalism of generalized parton distributions (GPDs) allows a consistent description of nucleon structure. In different limiting cases the GPDs incorporate the well-known nucleon form factors determined from elastic scattering as well as parton distribution functions (PDFs) determined from measurements of inclusive and semi-inclusive deep inelastic lepton-nucleon scattering (DIS and SIDIS respectively). Strong interest in the GPD framework has also evolved because of the fact that GPDs encode the unknown total angular momentum of quarks and gluons within the nucleon (J_q and J_g respectively). With the knowledge of the quarks' spin contribution to the spin of the nucleon, knowledge of the GPDs allows in principle also access to the orbital angular momentum of quarks (L_q) [2].

The theoretically cleanest process to constrain GPDs is Deeply-Virtual Compton Scattering (DVCS), in which a highly virtual photon (emitted by the incoming lepton beam) is absorbed by a parton of the target nucleon and produces a single real photon in the final state along with the recoiling nucleon in its ground state.

2 DVCS at HERMES

The DVCS process has the same final state as the Bethe-Heitler (BH) process, in which a real photon is radiated by either the incoming or the outgoing lepton. As this makes both processes experimentally indistinguishable, the cross section for leptonproduction of real photons is therefore given by the coherent sum of the DVCS and BH amplitudes squared:

$$d\sigma \propto |\tau_{\text{DVCS}}|^2 + |\tau_{\text{BH}}|^2 + \underbrace{\tau_{\text{DVCS}}^* \tau_{\text{BH}} + \tau_{\text{DVCS}} \tau_{\text{BH}}^*}_I \quad (1)$$

At HERMES kinematics the BH process is the dominant contribution to the cross section. However, the DVCS amplitude can be accessed via the interference term (I) by measuring various cross section asymmetries and their dependence on the azimuthal angle ϕ , which is

defined as the angle between the lepton scattering plane and the photon production plane. The interference term can be expressed as a series of Fourier moments in the angle ϕ : [3]

$$I \propto \pm \left(c_0^I + \sum_{n=1}^3 c_n^I \cos(n\phi) + \sum_{n=1}^3 s_n^I \sin(n\phi) \right), \quad (2)$$

where the + or - sign is used in case of an electron or positron beam respectively and where c_0^I, c_n^I, s_n^I represent linear combinations of the Compton form factors (CFFs) which in general depend on the beam helicity and the target polarization. The GPDs themselves are convolutions of hard scattering kernels with these CFFs.

By measuring with different beam charge and helicity states and with different target polarizations (longitudinal and transverse), HERMES accesses both the real and imaginary parts of the CFFs \mathcal{H} , \mathcal{E} , $\tilde{\mathcal{H}}$ and $\tilde{\mathcal{E}}$ and thus the corresponding GPDs. At leading order and leading twist the expressions for the cross section differences which give rise to beam-charge (BCA), beam-spin (BSA), longitudinal target-spin (LTSA) and the transverse target-spin (TTSA) asymmetries are

$$\begin{aligned} d\sigma(e^+, p) - d\sigma(e^-, p) &\propto \cos(\phi) \operatorname{Re}[F_1 \mathcal{H}] \\ d\sigma(\vec{e}, p) - d\sigma(\overleftarrow{e}, p) &\propto \sin(\phi) \operatorname{Im}[F_1 \mathcal{H}] \\ d\sigma(e, \overleftarrow{p}) - d\sigma(e, \vec{p}) &\propto \sin(\phi) \operatorname{Im}[F_1 \tilde{\mathcal{H}}] \\ d\sigma(\phi, \phi_S) - d\sigma(\phi, \phi_S + \pi) &\propto \sin(\phi - \phi_S) \cos(\phi) \operatorname{Im}[F_2 \mathcal{H} - F_1 \mathcal{E}] + \\ &\quad \cos(\phi - \phi_S) \sin(\phi) \operatorname{Im}[F_2 \tilde{\mathcal{H}} - F_1 \xi \tilde{\mathcal{E}}]. \end{aligned} \quad (3)$$

Here ϕ_S is the angle between the lepton scattering plane and the target polarization vector, ξ is the skewedness parameter defined as $\approx \frac{x_B}{2-x_B}$, and F_1 and F_2 are the Dirac and Pauli form factors of the proton respectively.

3 The Experiment

HERMES is a fixed target experiment that uses the 27.6 GeV electron and positron beam provided by HERA [4]. To extract the above mentioned asymmetries from the data, events were selected that contained exactly one photon and one lepton track (the latter with charge equal to the beam charge). Lepton-hadron identification is performed by a transition-radiation detector, a preshower counter and an electromagnetic calorimeter. Photons were identified by their large energy deposit in the calorimeter and preshower counter along with the absence of a corresponding track in the drift and proportional chambers. The cuts imposed on the lepton kinematics were: $Q^2 > 1 \text{ GeV}^2$, $W > 3 \text{ GeV}$. The angle $\theta_{\gamma^* \gamma}$ between the virtual and real photon was limited to range between 5 and 45 mrad.

For the data collected up to 2005, the recoiling proton was not detected. Exclusive DVCS events were therefore selected by applying a cut on the missing mass M_X . The exclusive region was defined as $-(1.5 \text{ GeV})^2 < M_X^2 < (1.7 \text{ GeV})^2$.

4 Transverse Target-Spin Asymmetry

The transverse target-spin asymmetry associated with DVCS on the proton can be measured with an unpolarized lepton beam (U) and a transversely polarized (T) hydrogen target [5].

The quark's total angular momentum J_q ($q = u, d$) can be accessed through a GPD model [6] that uses J_u and J_d as free parameters to parametrize the GPD E . Within this model the TTSA amplitude $A_{UT}^{\sin(\phi-\phi_S)\cos(\phi)}$ is found to be sensitive to J_u and J_d . Figure 1 shows the TTSA amplitudes $A_{UT}^{\sin(\phi-\phi_S)\cos(\phi)}$ and $A_{UT}^{\cos(\phi-\phi_S)\sin(\phi)}$ as a function of $-t$, x_B and Q^2 extracted from the HERMES data collected in 2002-2004. The curves in the figure represent predictions from a GPD model with different u -quark total angular momentum J_u and fixed d -quark total angular momentum $J_d = 0$ [5]. The first amplitude ($A_{UT}^{\sin(\phi-\phi_S)\cos(\phi)}$) shows the expected sensitivity to J_u and was used to obtain a first model-dependent constraint on a linear combination of J_u and J_d . The reduced χ^2 value, defined as

$$\Delta\chi^2 \equiv \chi^2 - \chi_{\text{minimum}}^2 = [A^{\text{exp}} - A^{\text{VGG}}(J_u, J_d)]^2 / [\delta A_{\text{stat}}^2 + \delta A_{\text{sys}}^2] \quad (4)$$

is evaluated on a J_u, J_d grid. Here A^{exp} is the measured TTSA amplitude integrated over the kinematic range of the data, δA_{stat} (δA_{sys}) is the statistical (systematic) uncertainty, and A^{VGG} is the value calculated at the average kinematics of the measurement by a code [7] based on the mentioned GPD model [6]. The area in the (J_u, J_d) -plane, in which the reduced χ^2 value is not larger than one, is defined as the one-standard-deviation constraint on J_u vs. J_d and shown in Figure 2. The constraint can be parametrized as $J_u + J_d/2.9 = 0.42 \pm 0.21 \pm 0.06$, where the first uncertainty denotes the experimental uncertainty in the measured TTSA amplitude, whereas the second one is a model uncertainty from the unknown profile parameter b [6]. The D-term contribution to the GPDs H and E is set to zero, as suggested by the HERMES results on the beam charge asymmetry (BCA).

5 The Recoil Detector

In late 2005, a recoil detector was installed at HERMES. It allows the detection of the recoiling proton and therefore greatly reduces the background contribution in the exclusive

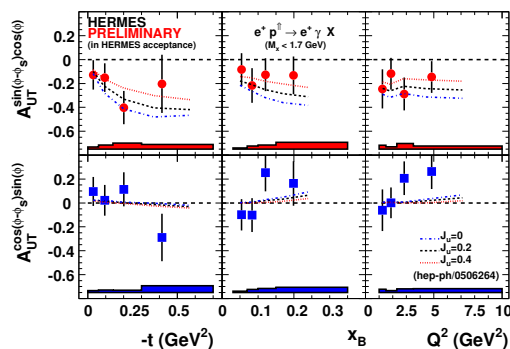


Figure 1: The TTSA amplitudes $A_{UT}^{\sin(\phi-\phi_S)\cos(\phi)}$ and $A_{UT}^{\cos(\phi-\phi_S)\sin(\phi)}$ as a function of $-t$, x_B and Q^2 .

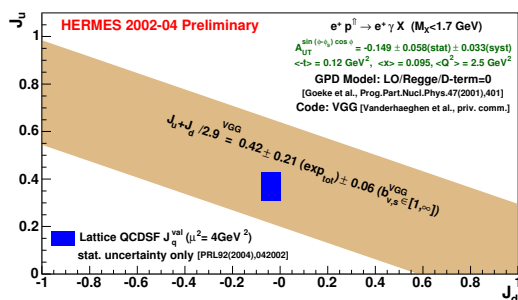


Figure 2: Model-dependent constraint on J_u and J_d . The lattice result from the QSDSF collaboration is also shown.

missing mass region. This background is due to associated BH with an intermediate Δ -resonance and to semi-inclusive processes and is reduced from about 15 % to below 1 % by the recoil detector.

The detector basically consists of three sub-detectors. The innermost is a two-layer silicon detector arranged in a diamond-like shape around the target cell inside the HERA beam vacuum at a distance of only 5 cm from the beam. It allows a precise measurement of the deposited energy and provides coordinate input for particle tracking. Outside the vacuum, two barrels with scintillating fibers provide additional input for the momentum reconstruction and measure the energy deposition of particles. The third sub-detector is a photon detector consisting of 3 layers of tungsten and scintillator. The whole detection system is enclosed in 1 T superconducting solenoid.

For low momentum particles the momentum is reconstructed by the silicon detector via the sum of the energy losses (for stopped particles) and dE/dx for particles punching through both silicon detection layers. Higher momentum particles are reconstructed via the bending in the 1 T magnetic field. The tracked particles are identified by the individual energy deposits in the silicon detectors and the fiber tracker for particle momenta below 0.6 GeV/c. Figure 3 shows the good separation between protons and positive pions. For momenta above 0.6 GeV/c the additional energy loss information from the photon detector is used. Photons from π^0 decay are identified by the photon detector in the absence of a charged track reconstructed in the recoil detector.

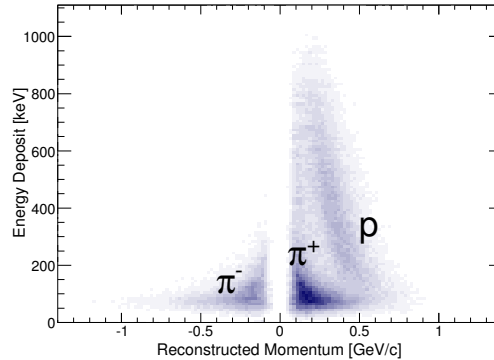


Figure 3: Energy deposit in the inner silicon detector vs. reconstructed momentum.

Acknowledgments

This work has been supported by the German Bundesministerium für Bildung und Forschung BMBF (contract nr. 06 ER 125I and 06 ER 143) and the European Community-Research Infrastructure Activity under the FP6 “Structuring the European Research Area” program (HadronPhysics I3, contract nr. RII3-CT-2004-506078).

References

- [1] Slides:
<http://indico.cern.ch/contributionDisplay.py?contribId=88&sessionId=12&confId=9499>
- [2] X. Ji, Phys. Rev. Lett. **78** 610 (1997); Phys. Rev. **D55** 7114 (1997).
- [3] A. V. Belitsky, D. Müller and A. Kirchner, Nucl. Phys. **B269** 323 (2002)
- [4] HERMES Coll., K. Ackerstaff *et al.*, Nucl. Instr. and Meth. **A417** 230 (1998)
- [5] F. Ellinghaus *et al.*, Eur. Phys. J. **C46** 729 (2006)
- [6] K. Goeke *et al.*, Prog. Part. Nucl. Phys. **47** 401 (2001)
- [7] M. Vanderhaeghen, P. A. M. Guichon and M. Guidal, priv. comm. (2003)